Title

Magnetic Resonance Imaging of the Globe-Tendon Interface for Extraocular Muscles: Is There an Arc of Contact?

Authors

Demer, Joseph
Clark, Robert

Publication Date

2018-10-01

DOI

10.1016/j.ajo.2018.07.002

Peer reviewed

HHS Public Access

Author manuscript

Am J Ophthalmol. Author manuscript; available in PMC 2019 October 01.

Published in final edited form as:

Am J Ophthalmol. 2018 October ; 194: 170–181. doi:10.1016/j.ajo.2018.07.002.

Magnetic Resonance Imaging of the Globe-Tendon Interface for Extraocular Muscles: Is there an "Arc of Contact"? (An American Ophthalmological Society Thesis)

Robert A. Clark, MD[1,5] and **Joseph L. Demer, MD, PhD**[1,2,3,4,5]

[1]Departments of Ophthalmology University of California, Los Angeles

[2]Departments of Neurology University of California, Los Angeles

[3]Departments of NeuroscienceUniversity of California, Los Angeles

[4]Departments of Biomedical Engineering Interdepartmental Programs University of California, Los Angeles

[5]Departments of David Geffen Medical School, University of California, Los Angeles

Abstract

PURPOSE: To determine if the "arc of contact" is an accurate approximation of the globe-tendon interface for the biomechanical modeling of extraocular muscle (EOM) force transfer onto the globe.

METHODS: At a single academic institution, 18 normal and 14 strabismic subjects were prospectively recruited for surface-coil enhanced magnetic resonance imaging at 312- or 390-micron resolution in axial planes for horizontal EOMs (23 subjects, 26 orbits) and sagittal planes for vertical EOMs (13 subjects, 22 orbits) during large ipsiversive ductions. The measured angle at insertion and the predicted angle assuming an "arc of contact" were compared using paired t-tests.

RESULTS: For normal EOMs, the measured angle at insertion was significantly greater than predicted assuming an "arc of contact" for the medial rectus (MR) (5.0° ± 4.8° versus 0.0° ± 0.0°, *P*=.03), lateral rectus (LR) (4.9° ± 3.0° versus 0.0° ± 0.0°, *P*=.02), inferior rectus (7.4° ± 4.8° versus 1.2° ± 2.6°, *P*=.00003), and superior rectus (0.6° ± 1.1° versus 0.0° ± 0.0°, *P*=.04). In strabismic subjects, the measured angle was significantly greater for the MR in abducens palsy (9.9° ± 4.3° versus 0.5° ± 0.7°, *P*=.0007) and after MR resection (9.0° ± 6.9° versus 1.2° ± 2.4°, *P*= .02), but not after LR recession (2.9° versus 0.0°). Single subjects had comparable angles after MR recession, but markedly different angles after MR and LR posterior fixation.

CONCLUSIONS: Contrary to the "arc of contact" biomechanical model, normal and post-surgical EOMs are significantly non-tangent to the globe at their scleral insertions. The "arc of

Address for Correspondence and Reprint Requests: Robert A. Clark, MD, 4100 Long Beach Blvd, Suite 108, Long Beach, CA 90807, (562) 426-3925 (voice); (562) 595-1375 (fax); drraclark@gmail.com.

C. *Contributions of Authors in each of these areas*: Design and conduct of the study (RAC, JLD); collection, management, analysis, and interpretation of the data (RAC, JLD); and preparation, review, and approval of the manuscript (RAC, JLD).

DISCLOSURES

B. *Financial Disclosures*: Dr. Clark reports personal fees from Nevakar, LLC, outside the submitted work.

contact" should be replaced in biomechanical modeling by the experimentally measured angles at tendon insertions.

INTRODUCTION

The functional anatomy of the rectus extraocular muscles (EOMs) is divided into two portions. The anterior part incorporates the collagenous tendon insertion and a portion of the contractile muscle wrapping in contact with the scleral surface, while the posterior part incorporates contractile muscle not contacting the scleral surface but extending from it to the muscle origin at the orbital apex. When devising mechanical schemes of orbital mechanics to explain the effects of strabismus surgery on ocular motility, researchers have traditionally relied upon planar Euclidean geometry to simplify analysis.[1–4] More recent studies have incorporated the presence of the EOM pulleys that define EOM posterior paths,[5, 6] but still rely upon the concept that EOMs wrap over the globe surface for a distance described as the "arc of contact" to define both the point of application and direction of the force applied by each EOM onto the globe.[7, 8] The "arc of contact" biomechanical model, in turn, relies upon two additional assumptions: first, that each EOM tendon can be treated biomechanically as an infinitely thin line of force that wraps around globe and applies all of the EOM's force as oculorotary until its insertion shifts far enough posteriorly during ocular rotation that the EOM tendon loses tangency with the sclera; and second, that the posterior EOM path is a straight line between the point of globe tangency and the EOM's anatomical origin. Using this simplified model (Figure 1 Left), once the EOM insertion rotates beyond the "arc of contact" to lose tangency with the globe, the oculorotary lever arm is reduced to less than the globe radius,[1, 3] resulting in loss of oculorotary torque.

The foregoing simplistic biomechanical model has often been invoked to define important principles presumably applicable to strabismus surgery, such as the maximum recession that can be safely performed before crippling an EOM[4] or explaining the mechanical effects of posterior fixation surgery.[3, 7, 9, 10] Even casual inspection, however, of in vivo anatomy in normal subjects using magnetic resonance imaging (MRI) (Figures 2 and 3) reveals that EOMs are not infinitely thin and their paths are not linear. Instead, the tendinous insertions are approximately one mm thick[11] and the EOM paths are curvilinear, deflected from a straight-line path by both EOM muscle bulk and orbital pulley tissue.[12, 13] The combination of tendon thickness at insertion and a curvilinear path prohibit perfect tangency of the EOM with the globe at any point (Figure 1 Right), even along what has traditionally been assumed to be its putative "arc of contact." The basic assumptions underlying the "arc of contact" biomechanical model are thus violated, but the magnitude of the discrepancy have been presumed small and may not be biomechanically relevant.

Abnormalities in the position and strength of the posterior functional anatomy of the rectus muscles, such as the heterotopic pulleys found in craniosynostosis syndromes and other anatomic disorders that create pattern strabismus[14–16] or the sagging lateral rectus (LR) EOM path that occurs with age[17, 18] or high myopia to create acquired esotropia and hypotropias[19, 20], have been well described and analyzed. Abnormalities in the anterior EOM anatomy have also been described, although the emphasis has been on incomplete or imperfect re-attachment after surgical repositioning[21, 22] rather than the thickness and angle

of tendinous attachment. To the clinician, securing a firm and permanent re-attachment of the rectus muscle to the globe is of paramount concern after surgery. To the scientist, understanding the biomechanics of the tendinous attachment is equally important, especially when considering the effects of introducing materials around the insertion like amniotic membranes to reduce scarring and adhesions[23]. In this study we used MRI to measure the actual angle at tendon insertion to determine if the “arc of contact” model, while not a perfect characterization of the globe-tendon interface, still provides a reasonably accurate estimate of EOM force transference onto the globe.

METHODS

We conducted this study at a single academic institution as a prospective observational series. Each participant gave written informed consent to a protocol approved by the Institutional Review Board at the University of California, Los Angeles that conformed to the Declaration of Helsinki. The data collection was Health Insurance Portability and Accountability Act compliant.

Eighteen normal adult subjects (9 males and 9 females) ages 22–74 (average 50.1 yrs) were recruited through advertisement and were examined to verify normal vision, motility, and ocular structures. Fourteen strabismic subjects (6 males and 8 females) ages 19–75 (average 48.6 yrs) were recruited as part of an ongoing prospective imaging study: seven subjects with chronic unilateral LR palsy, five subjects with horizontal strabismus status post horizontal strabismus surgery, and two subjects following posterior fixation suture placement. Imaging for the two subjects with posterior fixation sutures has been previously reported using different analytical techniques as part of a study on the mechanics of posterior fixation surgery.[7] In both cases, posterior fixation was performed using interrupted permanent sutures placed through the sclera and adjacent superior and inferior poles of the operated rectus muscle far posterior to the muscle’s insertion to shift the muscle’s functional position of globe tangency to the location of the sutures instead of its tendinous insertion onto the globe[7].

High-resolution, T1- or T2-weighted fast spin echo MRI was performed on each subject with a 1.5-T General Electric Signa (Milwaukee, WI) scanner utilizing techniques described in detail in prior studies.[24–27] In brief, subjects were scanned in the supine position with the head encased within foam cushions. Gaze was controlled using a fixation target, a fine optical fiber embedded in a plastic facemask located 2 cm in front of the scanned eye and illuminated from its distal end by a red light emitting diode that was positioned to create large ipsiversive globe rotations towards the EOM of interest, i.e. maximal adduction for scans of the medial rectus (MR). A dual-phased surface coil array (Medical Advances, Milwaukee, WI) was positioned over the scanned orbit to improve the signal-to-noise ratio (this surface coil has not been not approved by the US Food and Drug Administration for this purpose).

Axial image planes were used to evaluate the horizontal rectus EOMs (Figure 2 Left) and quasi-sagittal image planes, vertically transecting the orbit along its long axis, were used to evaluate the vertical rectus EOMs (Figure 2 Right). Imaging was performed using a matrix

of 256 pixels over an 8- or 10-cm field of view, yielding a pixel resolution of 312- or 390-microns, respectively. Digital MRI images were quantified using the program *ImageJ64* (W. Rasband, National Institutes of Health, Bethesda, MD, http://rsb.info.nih.gov/ij/, 1997–2009).

For each subject in each relevant gaze position, an image plane that included the cornea and lens was analyzed to determine globe rotation into the scanned EOM's field of gaze (Figure 2). Each axial image was rotated to bring the midline of the nose to scanner vertical. The rotation of the globe into horizontal gaze was then measured on axial images as the angle displacement from scanner vertical of a line from the center of the cornea bisecting the lens through to the posterior globe. Similarly, the change in vertical gaze was measured on sagittal images as the angle displacement from scanner horizontal of a line from the center of the cornea bisecting the lens through to the posterior globe. The globe center was approximated by manually outlining the globe and using the ImageJ "Area Centroid" measurement (Figure 2). To reduce the aspheric effect of corneal curvature, the posterior aspect of the cornea was used to delineate the anterior extent of the globe for this measurement.

Then, a single axial or sagittal image plane was chosen for angle measurements that contained the entirety of the rectus EOM, origin to insertion. To perform the angle measurements, the globe center was marked directly on each image with a single white pixel (labeled "1" in all figures). Then, three additional white pixels were placed on each image. The second white pixel marked the point of EOM insertion (labeled "2" in all figures) and the third white pixel bisected the EOM tendon a short distance posterior to the insertion (labeled "3" in all figures), where the muscle path still appeared linear from the insertion. The angle between the globe center (1), EOM insertion (2), and EOM tendon (3) was then measured in *ImageJ64* and used to calculate the actual angle at tendon insertion, defined as the measured angle minus the 90-degree angle formed by a perfect globe tangent (Figures 3 and 4). The final white pixel bisected the posterior EOM belly near its origin in the posterior third of the orbit (labeled "4" in all figures). The angle between the globe center (1), EOM insertion (2), and posterior EOM belly (4) was used to calculate the predicted angle at insertion from the "arc of contact" biomechanical model (Figures 3 and 4). If this "arc of contact" angle was less than 90 degrees, possible because the curve of the EOM around the globe was neglected for this measurement, this angle was defined as zero degrees (a perfect tangent to the globe). If the angle exceeded 90 degrees, the "arc of contact" angle was calculated as this angle minus 90 degrees.

For normal subjects and subgoups of strabismic patients with sufficient numbers for analysis, the measured angle at tendon insertion was compared with the predicted "arc of contact" angle using paired t-tests. Data from individual strabismic subjects was also included for descriptive purposes.

RESULTS

On imaging, the EOMs could be tracked from near the origin to the insertion for every subject. At the insertion, the thickness of the tendon created a measurable angle at tendon

insertion for most EOMs, regardless of posterior path (Figures 2, 3 and 4). Each of the posterior EOM bellies had one of two distinct morphologies. The MR and inferior rectus (IR) had thicker, fusiform bellies that tapered into comma-shaped, curved tendons. During contraction, the MR tendon flattened somewhat towards the globe, slightly decreasing the angle at tendon insertion, while the IR tendon retained most of its retroequatorial curve. The superior rectus (SR) and lateral rectus (LR) had a smoother curvilinear course from origin to insertion, with no marked taper or curve within the tendon compared with the EOM belly. For both of those EOMs, the posterior muscle path straightened markedly with contraction.

For each EOM in normal subjects, the measured angle at tendon insertion was significantly greater than the “arc of contact” angle, demonstrating a greater loss of muscle tangency than predicted by the “arc of contact” model even for normal EOMs during routine gaze changes. Figure 3 displays representative images for each normal EOM. For the MR in adduction (5.0° ± 4.8° measured versus 0.0° ± 0.0° predicted, $P = .03$), LR in abduction (4.9° ± 3.0° versus 0.0° ± 0.0°, $P = .02$), and IR in infraduction (7.4° ± 4.8° versus 1.2° ± 2.6°, $P = .00003$), both the average and maximum measured angles at tendon insertion differed substantially from the angles predicted by the “arc of contact” model. For the SR in supraduction, both the average angle at insertion (0.6° ± 1.1°versus 0.0° ± 0.0°, $P = .04$) and the maximum angle of 3.6°, while statistically significantly different than predicted, were too small to be biomechanically significant. Not all positions of gaze were imaged in each normal subject, but sufficient images were available to generate statistically significant results for all rectus EOMs. Results for the normal subjects are summarized in Table 1.

The clinical data for the subjects undergoing horizontal strabismus surgery are summarized in Table 2. Comparable results for the measured angle at tendon insertion for strabismic patients are summarized in Table 3. Statistical comparisons could only be performed for two subgroups, both involving the MR. In patients who had LR palsy with a resultant large esotropia (ET), the MR had a significantly larger angle at insertion (9.9° ± 4.3°) than predicted from the ‘arc of contact” model (0.5° ± 0.7°, $P = .0007$). For this group with paralytic ET, the measured angle was almost double that found in the normal MR during adduction, despite similar degrees of adduction for both groups (Figure 4 Upper Left). Unexpectedly, the MR after large resection for exotropia also had a significantly larger angle at insertion (9.0° ± 6.9°) than predicted from the ‘arc of contact” model (1.2° ± 2.4°, $P = .02$), similar to the finding in LR palsy (Figure 4 Upper Right). Because the MR tendon insertion was in the normal anatomic location for both of these strabismic groups, this finding suggests that increased EOM bulk at the insertion, either from intrinsic contracture after paralysis of the antagonist or from anterior shift of the EOM belly after surgical resection, substantially increases the angle at tendon insertion with subsequent loss of MR tangency to the globe.

On the other hand, the LR after large recessions for both subjects had smaller measured angles at tendon insertion than occurred in normal subjects during abduction for both subjects, despite retroplacement of the insertion 7 to 9 mm (Figure 4 Center Left). The only patient who underwent bilateral MR recessions of 6.5 mm had similar measured and predicted angles at tendon insertions (Figure 4 Center Right).

The only subject with a substantially smaller measured angle at tendon insertion than predicted from the ‘arc of contact” model had undergone MR scleral posterior fixation (Figure 4 Lower Left). Using this measurement technique, both the “arc of contact” and actual angles were smaller than those reported in the prior study,[7] but the conclusions are the same – the actual loss of MR tangency during ipsiversive duction after posterior fixation was not as large as predicted and, in fact, fell within the range found for the normal MR during adduction. The angle at tendon insertion after LR scleral posterior fixation was slightly larger than the predicted angle, but also fell within the range for the normal LR during abduction (Figure 4 Lower Right). Overall, the maximum loss of oculorotary force from the angle at tendon insertion, based on force vector analysis and the cosine of the measured angle, was less then 7% for all subjects.

DISCUSSION

For all normal and most strabismic subjects, during ipsiversive ductions the angle at scleral tendon insertion was significantly larger, producing greater loss of muscle tangency, than predicted by the “arc of contact” biomechanical model. Two factors were visible on MRI that accounted for the difference: EOM tendon thickness, particularly pronounced after surgical resection and somewhat diminished after surgical recession (Table 3), and the curvilinear posterior EOM path. Only one subject had a substantially smaller measured angle than predicted. For this subject who underwent MR posterior fixation with scleral sutures, the curvilinear posterior MR path eliminated some of the predicted effects of the posterior fixation (Figure 4 Lower Left).[2, 3] Given the current practicality and widespread availability of noninvasive high-resolution orbital imaging, this data strongly suggests that the “arc of contact” be abandoned and replaced in biomechanical modeling by the experimentally measured angles at tendon insertion. Conclusions that rely exclusively on line-drawn biomechanics[1–4, 8] should require in vivo confirmation prior to widespread acceptance to ensure that the actual EOM tendon anatomy matches the schematic anatomy.

Clearly, it is overly simplistic to model the EOM insertion as a single point and the EOM tendon as infinitely thin. The high-resolution MRI used for this study allowed identification of the EOM insertion in these subjects, but did not allow direct visualization of the individual muscle fibers that comprise the force generating units within each EOM. These fibers are parallel throughout most of the EOM belly, but cannot follow exactly parallel straight lines at the EOM insertion. Instead, the most posterior fibers are tangent to the globe at scleral contact, while the more anterior fibers lose tangency as they curve from scleral attachment around the posterior fibers to complete the EOM tendon (Figure 1 Right). The transmission of EOM force to the globe is thus made less efficient and, even in normal subjects, never achieves the perfect globe tangency predicted by the “arc of contact” model. From angle at tendon insertion measurements only, the maximum loss of oculorotary force was less then 7% for all subjects based upon force vector analysis and the cosine of the measured angle. In strabismic subjects, however, the relative size, number, orientation, and distribution of fibers at EOM insertion may vary with pathology, surgical technique, orbital anatomy, or other factors and further diminish the oculorotary effectiveness of the EOM.

The most directly comparable MRI study of the “arc of contact” is by Chatzistefanou and coworkers.[28] That study utilized MRI to measure the length of scleral contact for each EOM and equated that length directly with the “arc of contact” concept. Those authors made the fundamental assumption that scleral contact equals perfect tangency, an assumption disproven by their own Figures 1 through 5. Their post-surgical Figures 4 and 5, in particular, depict substantial tendon thickening anteriorly that markedly increased the angle at tendon insertion and thus reduced the oculorotary effectiveness of the operated EOM, “scleral contact” notwithstanding. That study’s main conclusion, that EOM-sclera contact is required after surgery to promote re-attachment of the EOM tendon to the globe, remains valid, but should not be confused with the “arc of contact” biomechanical model of perfect globe tangency that transmits all the EOM force as oculorotary.

This data continues to expand our understanding of the biomechanics of eye movement by replacing assumed behavior with experimentally determined in vivo behavior. The most immediate impact is to improve the accuracy of mathematical models designed to predict changes in eye movements in response to various perturbations. Beginning with the seminal studies by Miller[5] and Demer[13, 29] almost 30 years ago, the combination of high resolution orbital imaging and careful orbital histology has profoundly influenced the fundamental principles governing eye movement. The connective tissue pulleys that constrain posterior EOM belly sideslip simplify neurological control of eye movements by solving the potentially complex mathematics of coordinated three-axis eye movements with an elegant mechanical solution[30, 31]. The pulleys themselves retract posteriorly with EOM contraction and extend anteriorly with EOM relaxation because a portion of each EOM, the orbital layer, inserts into the pulley itself[30, 31]. The shifts in pulley position mechanically implement the necessary change in rotational angle required by Listing’s Law of ocular torsion without requiring complex upper level neurological input[30, 31]. The brain can control eye movement with simple directional commands while the structure and behavior of the orbital tissues solves the complex mathematical relationships to ensure smooth, coordinated eye tracking and alignment.

The discovery of the pulleys has quickly progressed from basic science and computer simulations into clinical practice along three major lines: 1) improvements in existing surgical techniques; 2) recognition of the role of disorders in EOM pulley location in previously poorly defined pathology; and 3) creation of novel techniques to correct those disorders. One of the most important modifications to strabismus surgery in recent history has been the addition of posterior fixation sutures to augment the effects of transposition surgery[32]. These sutures are designed to transpose the posterior EOM belly to match the surgical transposition of the EOM insertion, an addition not considered necessary until the discovery of EOM pulleys. The posterior fixation sutures directly increase the mechanical force of the tendon transposition by shifting the EOM pulley itself[33], improving the mechanical effectiveness of transposition surgery so profoundly that transpositions augmented with posterior fixation have virtually supplanted all prior transposition techniques.

Abnormality of EOM pulley location has now been implicated in one of the leading forms of acquired adult strabismus, distance ET with normal near alignment. Imaging demonstrates

age-related dehiscence of the LR pulley suspension from the SR[17–19]. The LR pulley slides inferotemporally around the globe, changing the LR direction of force from directly temporal to inferotemporal. The displaced LR force is no longer sufficient to balance the MR adducting force in central gaze, resulting in ET and horizontal diplopia in the distance that resolves on near gaze when the diminished LR force is no longer biomechanically important. The posteriorly sagging LR belly that defines "sagging eye syndrome[17, 18]" can be directly treated with novel surgeries designed to correct the LR pulley displacement, such as loop myopexy[34] and LR equatorial myopexy[35], without changing the position of the LR insertion. This approach can reduce tissue trauma, future risk of healing abnormalities such as stretched scar or hypertrophic scar, and patient morbidity.

Another recent finding that has fundamentally altered our understanding of orbital biomechanics is the discovery that all EOMs except the SR have bifid, segregated neuromuscular innervation, essentially created two functionally distinct muscles within each EOM[36–38]. Rather than acting as a single, monolithic contractile force, the different poles of compartmentalized EOMs contract differentially to generate secondary rotational forces that are functionally important during various eye movements such as vertical vergence or ocular counter-rolling[39–42]. Similar to the discovery of EOM pulleys, recognition of EOM compartments has allowed the identification of a new clinical entity, compartmental EOM palsy[43, 44]. Rather than affecting the entire EOM, palsy of the superior compartment of the LR is associated with a smaller primary gaze ET, better abducting function, and an associated small vertical deviation that distinguishes it from the larger ET and profound abduction deficit created by a complete LR palsy affecting both LR compartments[43]. Similarly, superior oblique (SO) compartmental palsies primarily affect the lateral compartment, which contributes to vertical gaze, rather than the medial compartment, which contributes to torsion[44]. The presence of neuromuscular compartments supports an ongoing clinical role for partial EOM surgery such as split-tendon transpositions[45], slanted recessions[46–49], SO posterior tenectomy, and the Harada-Ito procedure[45]. Going forward, the identification of functional neuromuscular EOM compartments suggests an expanded role for more targeted strabismus surgery, focusing intervention on the compartment of the EOM most likely to correct the pathology while preserving the function and ciliary circulation of the other, uninvolved compartment.

By redefining the anatomy and biomechanics of the EOM insertions onto the globe, the angle at insertion will increase the precision of the biomechanical analysis and mathematical modeling of eye movements. The clinical impact of these findings is also becoming apparent. Recognition of the difference between the angle at insertion and perfect globe tangency has already led to a significant modification to an existing surgical technique. The most obvious example of the erroneous application of the "arc of contact" model was the biomechanical explanation for the use of posterior fixation sutures to limit a muscle's function into its field of gaze. Simple line drawings suggested that the posterior EOM insertion created by the scleral sutures would lose tangency with the globe during contraction, resulting in minimal effect in central gaze but significant muscle weakening during contraction[2, 3]. Imaging studies have demonstrated, however, that the actual loss of tangency is much less than predicted and, in fact, most of the mechanical effect impeding muscle contraction occurs due to a collision between the posterior scleral attachment and the

muscle's pulley sleeve[7]. This improved understanding of the mechanism of action resulted in a modification of the posterior fixation procedure to place the suture directly through the pulley sleeve instead of the sclera[50], resulting in a much safer procedure that accomplished similar results[25, 26].

The loss of MR tangency after surgical resection might also provide a biomechanical explanation for the effects of the combined recess-resect procedure (the same EOM is both resected and recessed simultaneously).[51–53] This procedure, touted as an easier and adjustable alternative to standard scleral posterior fixation, creates a bulky, retroplaced EOM-sclera attachment that, because of the increased tendon thickness at EOM insertion, could result in a greater loss of muscle tangency than predicted by the "arc of contact". The net result might be a stiffer, shortened EOM that maintains primary gaze alignment but whose tendon rapidly loses globe tangency during contraction. In vivo imaging after surgery is required to validate this prediction.

Beyond loss of EOM tendon tangency to the globe, post-surgical disorders of muscle fiber attachment onto the globe beyond slipped[22, 54] or stretched[21] muscles might also affect the angle at insertion. Tendon re-attachment to the globe after non-uniform (i.e. slanted recessions or partial tendon surgeries) might result in an oblique orientation of EOM fibers that would significantly reduce force transmission in the direction of EOM contraction despite apparently perfect insertional tangency with the globe. The resulting loss of EOM force should increase the effective recession effect of the surgery regardless of the direction of slant, thus providing a potential explanation for why EOM recessions slanted in opposite directions (i.e. MR superior pole anterior versus MR superior pole posterior) appear to create similar biomechanical effects[46].

There are three major limitations to the present study. The most important limitation is the imaging modality itself. High-resolution MRI clearly delineates the orbital structures, but for this purpose, the anatomy of the EOM beyond the first mm or two from its insertion is irrelevant. There is no need to define the middle of the posterior EOM (point 4 in the figures) because, just like the position of the posterior belly of the superior oblique (SO) plays no role in determining the pulling direction of the SO tendon, the position of the posterior rectus EOM belly plays no role in determining tendon-globe tangency. The immediate path of the tendon from its scleral attachment completely defines the direction of force application, so an imaging modality that provides greater resolution and a narrower field of view centered right at the EOM insertion might be more useful in defining the angle at tendon insertion by allowing characterization of the direction and organization of the individual muscle fibers as well as the breadth of the globe attachment. Ultrasound biomicroscopy has been used in the past to detect EOM insertions,[55–57] but may not have sufficient resolution to define the complete extent of the insertion, and is usually impossible during duction ipsiversive to the EOM of interest. Anterior segment optical coherence tomography (OCT) has shown considerable promise as a non-contact method of imaging the EOM insertion,[58] yet might share the anatomical limitation of UBM insofar as EOM insertions are displaced posteriorly and overlain by conjunctiva and other orbital tissues during large ipsiversive duction. Further investigation is required to determine if OCT can

provide useful anatomic data besides just detection of the EOM insertion site in contraversive gaze.

The second limitation is the lack of post-surgical imaging for the vertical rectus EOMs. The data on normal EOMs (Table 1) suggests that the inferior rectus (IR) might be most susceptible and the SR least susceptible to loss of globe tangency, in line with common clinical experience and prior imaging studies.[28] Post-surgical imaging after vertical rectus recessions and resections is required to confirm this prediction.

The final limitation is the small overall number of subjects, particularly strabismic subjects. In addition, the wide range of values for the measured angles at tendon insertion suggests that variation in EOM-scleral attachment may account for some of the variable results after strabismus surgery. More imaging is required to determine the magnitude of this effect.

CONCLUSION

In conclusion, MRI demonstrates that, contrary to the “arc of contact” biomechanical model, both normal and post-surgical EOMs are significantly non-tangent to the globe during large ipsiversive ductions. In most cases, the EOM tendon thickness and post-insertional curvilinear path combined to create a substantially larger than predicted angle at tendon insertion with resultant greater than predicted loss of globe tangency. From the angles measured in this study, the effective reduction in oculorotary force is less than 7%, but may be greater depending on the actual organization of the EOM tendon fibers at insertion. Past biomechanical modeling that relied exclusively on the “arc of contact” should be validated with imaging of the in vivo anatomy and future analyses of both normal and abnormal ocular motility should replace theoretical angles predicted by the “arc of contact” model with experimentally measured angles at tendon insertions.

ACKNOWLEDGEMENTS

A. *Funding/Support*: Grants EY008313 and EY000331 from the US Public Health Service, National Eye Institute and an unrestricted grant from Research to Prevent Blindness. The sponsors or funding organizations had no role in the design or conduct of this research.

REFERENCES

1. Beisner DH. Reduction of ocular torque by medial rectus recession. Arch Ophthalmol 1971;85(1): 13–17. [PubMed: 5539388]
2. Cuppers C The so-called “fadenoperation” (surgical corrections by well-defined changes of the arc of contact) In: Fells P, editor. The 2nd Congress of the International Strabismological Association. Marseille: Diffusion Generale de Librairie, 1976:395–400.
3. Scott AB. The faden operation: Mechanical effects. Am Orthop J 1977;2744–7.
4. Kushner BJ, Fisher MR, Lucchese NJ, Morton GV. How far can a medial rectus safely be recessed? J Pediatr Ophthalmol Strabismus 1994;31(3):138–46. [PubMed: 7931946]
5. Miller JM. Functional anatomy of normal human rectus muscles. Vision Res 1989;29(2):223–240. [PubMed: 2800349]
6. Clark RA, Miller JM, Demer JL. Location and stability of rectus muscle pulleys: Muscle paths as a function of gaze. Invest Ophthalmol Vis Sci 1997;38(1):227–240. [PubMed: 9008649]

7. Clark RA, Isenberg SJ, Rosenbaum AL, Demer JL. Posterior fixation sutures: a revised mechanical explanation based on rectus extraocular muscle pulleys. Am J Ophthalmol 1999;128(6):702–14. [PubMed: 10612506]
8. Miller AM, Mims JL. The influence of pulleys on the quantitative characteristics of medial rectus muscle recessions: The torque vector model. J AAPOS 2006;10(4):318–23. [PubMed: 16935230]
9. Shuckett EP, Hiles DA, Biglan AW, Evans DE. Posterior fixation suture operation (Fadenoperation). Ophthalmic Surg 1981;12(8):578–585. [PubMed: 7052555]
10. Guyton DL. The posterior fixation suture: Mechanism and indications. Int Ophthalmol Clin 1985;25(4):79–88. [PubMed: 3908360]
11. Apt L, Call NB. An anatomical reevaluation of rectus muscle insertions. Ophthalmic Surg 1982;13(2):108–12. [PubMed: 7110654]
12. Miller JM, Robins D. Extraocular muscle sideslip and orbital geometry in monkeys. Vision Res 1987;27(3):381–392. [PubMed: 3660599]
13. Demer JL, Miller JM, Poukens V, Vinters HV, Glasgow BJ. Evidence for fibromuscular pulleys of the recti extraocular muscles. Invest Ophthalmol Vis Sci 1995;36(6):1125–1136. [PubMed: 7730022]
14. Demer JL, Clark RA, Miller JM. Heterotopy of extraocular muscle pulleys causes incomitant strabismus In: Lennerstrand G, editor. Advances in Strabismology. Amsterdam: Swets, 1999:91–4.
15. Clark RA, Miller JM, Rosenbaum AL, Demer JL. Heterotopic muscle pulleys or oblique muscle dysfunction? J AAPOS 1998;2(1):17–25. [PubMed: 10532362]
16. Clark RA. The role of extraocular muscle pulleys in incomitant strabismus. Middle East Afr J Ophthalmol 2015;22279–85.
17. Demer JL, Chaudhuri Z, Clark RA. Apt Lecture Workshop: Cutting no slack for sagging eye syndrome. J AAPOS 2013;17(1):e33.
18. Chaudhuri Z, Demer JL. Sagging eye syndrome: Connective tissue involution causes horizontal and vertical strabismus in older patients. JAMA Ophthalmology 2013;131(5):619–25. [PubMed: 23471194]
19. Tan JRD, Demer JL. Heavy eye syndrome versus sagging eye syndrome in high myopia. J AAPOS 2015;19500–6.
20. Rutar T, Demer JL. “Heavy Eye” syndrome in the absence of high myopia: A connective tissue degeneration in elderly strabismic patients. J AAPOS 2009;13(1):36–44. [PubMed: 18930668]
21. Ludwig IH, Chow AY. Scar remodeling after strabismus surgery. J AAPOS 2000;4(6):326–33. [PubMed: 11124665]
22. Lenart TD, Lambert SR. Slipped and lost extraocular muscles. Ophthal Clin North Am 2001;14433–442.
23. Sheha H, Casas V, Hayashida Y. The use of amniotic membrane in reducing adhesions after strabismus surgery. J AAPOS 2009;13(1):99–101. [PubMed: 18976945]
24. Demer JL, Clark RA, Kono R, Wright W, Velez F, Rosenbaum AL. A 12-year prospective study of extraocular muscle imaging in complex strabismus. J AAPOS 2002;6(6):337–47. [PubMed: 12506273]
25. Clark RA, Ariyasu R, Demer JL. Medial rectus pulley posterior fixation is as effective as scleral posterior fixation for acquired esotropia with a high AC/A ratio. Am J Ophthalmol 2004;137(6): 1026–33. [PubMed: 15183786]
26. Clark RA, Ariyasu R, Demer JL. Medial rectus pulley posterior fixation: A novel technique to augment recession. J AAPOS 2004;8(5):451–6. [PubMed: 15492738]
27. Demer JL, Clark RA. Magnetic resonance imaging of human extraocular muscles during static ocular counter-rolling. J Neurophysiol 2005;94(5):3292–3302. [PubMed: 16033934]
28. Chatzistefanou KI, Kushner BJ, Gentry LR. Magnetic resonance imaging of the arc of contact of extraocular muscles: implications regarding the incidence of slipped muscles. J AAPOS 2000;4(2): 84–93. [PubMed: 10773806]
29. Miller JM, Demer JL. New orbital constraints on eye rotation In: Fetter M, Misslisch H, Tweed D, editors. Three-Dimensional Kinematic Principles of Eye-, Head-, and Limb Movements in Health and Disease. Tubingen: University of Tubingen, 1995:40.

30. Kono R, Clark RA, Demer JL. Active pulleys: magnetic resonance imaging of rectus muscle paths in tertiary gaze. Invest Ophthalmol Vis Sci 2002;432179–88.
31. Demer JL, Oh SY, Poukens V. Evidence for active control of rectus extraocular muscle pulleys. Invest Ophthalmol Vis Sci 2000;411280–90.
32. Foster RS. Vertical muscle transposition augmented with lateral fixation. J AAPOS 1996;1(1):20–30.
33. Clark RA, Demer JL. Rectus extraocular muscle pulley displacement after surgical transposition and posterior fixation for paralytic strabismus. Am J Ophthalmol 2002;133119–28.
34. Fresina M, Sapigni L, Benedetti C, Giannaccare G, Campos EC. Equatorial loop myopexy in "Sagging Eye" syndrome: a case report. Clin Exp Ophthalmol 2014;5(3):1000337.
35. Clark TY, Clark RA. Surgical correction of an inferiorly displaced lateral rectus with equatorial myopexy. J AAPOS 2016;20446–7.
36. Le A, Poukens V, Ying H, Rootman D, Goldberg RA, Demer JL. Compartmental innervation of the superior oblique muscle in mammals. Invest Ophthalmol Vis Sci 2015;566237–46.
37. da Silva Costa RM, Kung J, Poukens V, Yoo L, Tyschen L, Demer JL. Intramuscular innervation of primate extraocular muscles: Unique compartmentalization in horizontal recti. Invest Ophthalmol Vis Sci 2011;52(5):2830–6. [PubMed: 21220556]
38. Peng M, Poukens V, da Silva Costa RM, Yoo L, Tyschen L, Demer JL. Compartmentalized innervation of primate lateral rectus muscle. Invest Ophthalmol Vis Sci 2010;51(9):4612–7. [PubMed: 20435590]
39. Clark RA, Demer JL. Functional morphometry demonstrates extraocular muscle compartmental contraction during vertical gaze changes. J Neurophysiol 2016;115370–8.
40. Demer JL, Clark RA. Magnetic resonance imaging demonstrates compartmental muscle mechanisms of human vertical fusional vergence. J Neurophysiol 2015;1132150–63.
41. Demer JL, Clark RA. Magnetic resonance imaging of differential compartmental function of horizontal rectus extraocular muscles during conjugate and converged adduction. J Neurophysiol 2014;112845–55.
42. Clark RA, Demer JL. Differential lateral rectus compartmental contraction during ocular counter-rolling. Invest Ophthalmol Vis Sci 2012;53(6):2887–96. [PubMed: 22427572]
43. Clark RA, Demer JL. Lateral rectus superior compartment palsy. Am J Ophthalmol 2014;157479–87.
44. Suh SY, Clark RA, Le A, Demer JL. Extraocular muscle compartments in superior oblique palsy. Invest Ophthalmol Vis Sci 2016;575535–5540.
45. Rosenbaum AL, Santiago AP. Clinical Strabismus Management: Principles and Surgical Techniques. Philadelphia: W.B. Saunders Company, 1999:401–3.
46. Kushner BJ. Insertion slanting strabismus surgical procedures. Arch Ophthalmol 2011;1291620–5.
47. Choi M, Hwang J. The long-term result of slanted medial rectus resection in exotropia of the convergence insufficiency type. Eye 2006;201279–1283.
48. Snir M, Axer-Siegel R, Shalev B, Sherf I, Yassur Y. Slanted lateral rectus recession for exotropia with convergence weakness. Ophthalmology 1999;1069926.
49. Biedner B, Rothkoff L. Treatment for 'A' or 'V' pattern esotropia by slanting muscle insertion. Br J Ophthalmol 1995;79807–8.
50. Clark TY, Clark RA. Medial rectus pulley posterior fixation for esotropia with a high AC/A ratio. J AAPOS 2017;21(1):63. [PubMed: 28108346]
51. Bock CJ, Buckley EG, Freedman SF. Combined resection and recession of a single rectus muscle for the treatment of incomitant strabismus. J AAPOS 1999;3(5):263–8. [PubMed: 10532569]
52. Thacker N, Velez FG, Rosenbaum AL. Combined rectus muscle resection-recession for incomitant strabismus. J AAPOS 2005;9(2):137–40. [PubMed: 15838440]
53. Dawson E, Boyle N, Taherian K, Lee JP. Use of the combined recession and resection of a rectus muscle procedure in the management of incomitant strabismus. J AAPOS 2007;11(2):131–4. [PubMed: 17416322]
54. Rosenbaum AL, Metz HS. Diagnosis of lost or slipped muscles by saccade velocity measurements. Am J Ophthalmol 1973;77215–222.

55. Watts P, Smith D, MacKeen L, Kraft S, Buncic JR, Abdolell M. Evaluation of the ultrasound biomicroscope in strabismus surgery. J AAPOS 2002;6(3):187–90. [PubMed: 12075296]

56. Dai S, Kraft SP, Smith DR, Buncic JR. Ultrasound biomicroscopy in strabismus reoperations. J AAPOS 2006;10(3):202–5. [PubMed: 16814170]

57. Solarte CE, Smith DR, Buncic JR, Tehrani NN, Kraft SP. Evaluation of vertical rectus muscles using ultrasound biomicroscopy. 2008 2008;12(2):128–31.

58. Liu X, Wang F, Ziao Y, Zinhai Y, Lijie H. Measurement of the limbus-insertion distance in adult strabismus patients with anterior segment optical coherence tomography. Invest Ophthalmol Vis Sci 2011;52(11):8370–3. [PubMed: 21948556]

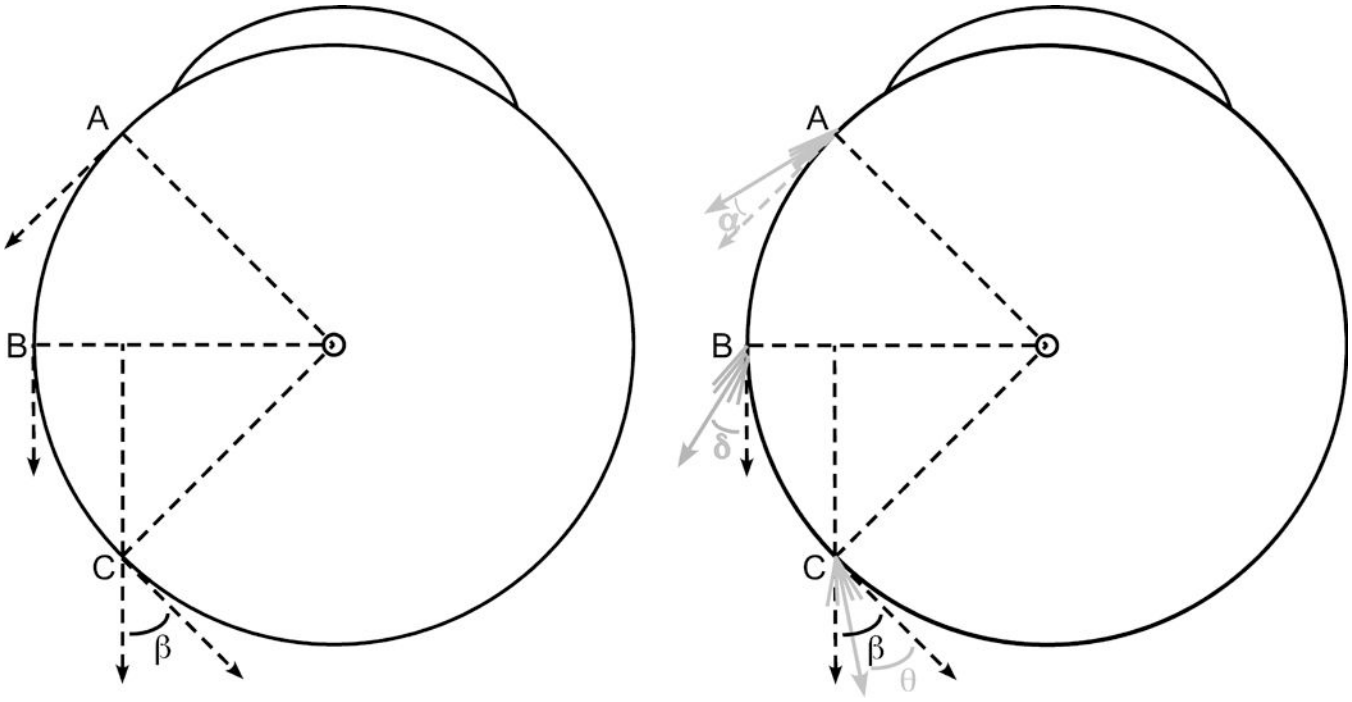

Figure 1:

Schematic diagram of the globe-tendon interface. Left) The "arc of contact" biomechanical model assumes infinitely thin extraocular muscle (EOM) tendons and linear muscle paths. As the EOM insertion rotates from point A to the equator (point B), perfect tangency is maintained with 100% force application as oculorotary torque. With further rotation from point B to point C, the posteriorly directed force is no longer tangent to the globe and some rotational torque is lost. The remaining oculorotary torque is proportional to the cosine of angle β. Right) The thickness of the tendon and the changes that occur in the posterior muscle belly during contraction fundamentally alter the globe-tendon interface. Instead of a single line at the EOM insertion, multiple lines are drawn to simulate the muscle fibers that thicken the insertion. At point A, the cumulative force from these lines can be summed into a single force vector displaced by angle α from perfect tangency. From the cosine function, for small angles α, almost 100% of the force exerts oculorotary torque. As the EOM insertion rotates from point A to point B, the muscle thickness increases with EOM contraction, resulting in a larger angle δ displacement from perfect tangency ($\delta > \alpha$). Finally, from point B to point C, imaging demonstrates that the EOM insertion begins to compress the pulley tissue, deforming the EOM path towards the center of the orbit. Thus, despite further thickening of the EOM belly, the resultant angle θ has been shown to be less than the angle β defined by the traditional "arc of contact" model[7] ($\theta < \beta$).

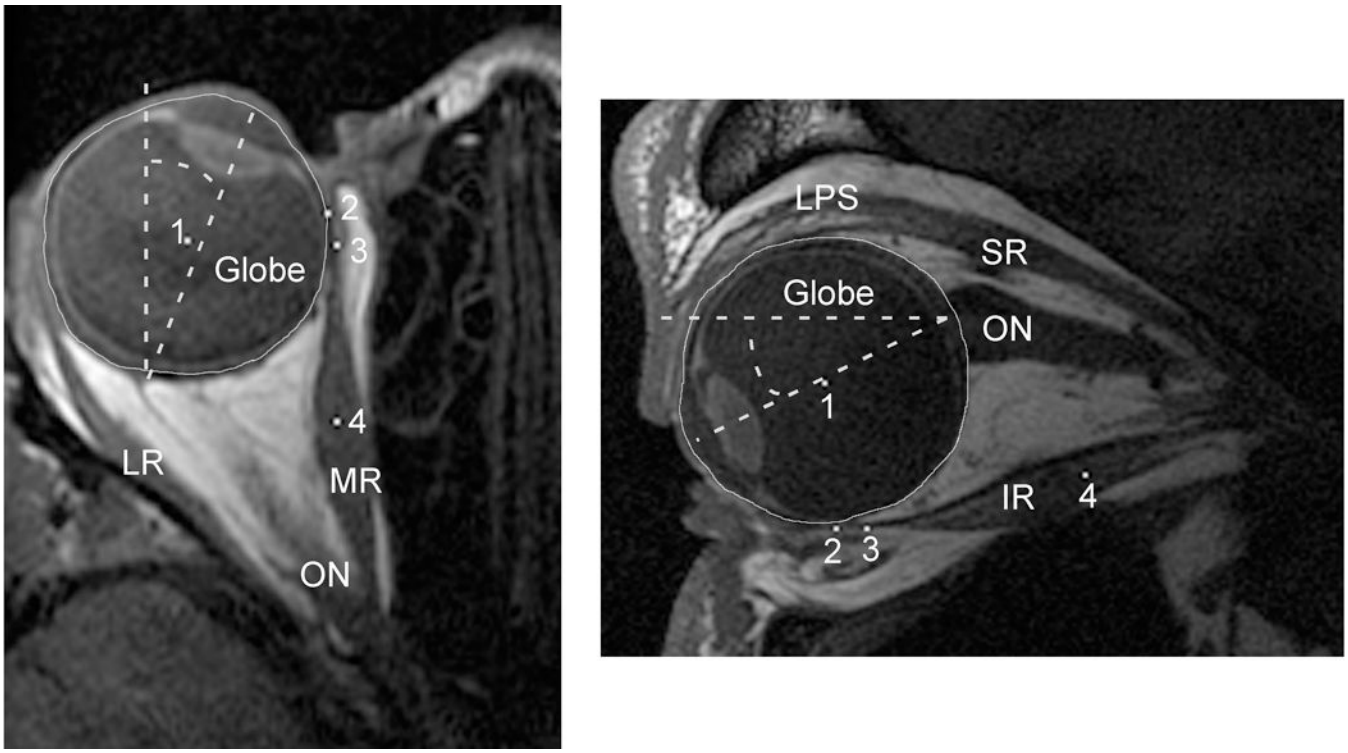

Figure 2:

Axial and quasi-sagittal magnetic resonance imaging (MRI) of the orbit. Left) Axial images were rotated to bring the midline of the nose to scanner vertical. The angle of globe rotation into adduction or abduction was then measured by drawing a line from the center of the cornea through the center of the lens towards the posterior globe and measuring the angle displacement of that line from scanner vertical (dashed lines). The center of the globe, marked with a white pixel (1), was determined by manually outlining the globe, then using the "Area Centroid" function of *ImageJ64* to find its center. The posterior aspect of the cornea was used to delineate the globe's anterior extent for this measure. White pixels were also used to mark the extraocular (EOM) insertion (2), immediate posterior tendon path (3), and middle of the posterior EOM belly (4). Right) For quasi-sagittal MRI, the angle of globe rotation into infraduction or supraduction was measured by a drawing a line from the center of the cornea through the center of the lens towards the posterior globe and measuring the angle displacement of that line from scanner horizontal (dashed lines). The center of the globe (1), EOM insertion (2), immediate posterior tendon path (3), and center of the posterior EOM belly (4) were defined the same as for the axial MRI. LR = Lateral Rectus; MR = Medial Rectus; ON = Optic Nerve; LPS = Levator Palpebrae Superioris; SR = Superior Rectus; IR = Inferior Rectus.

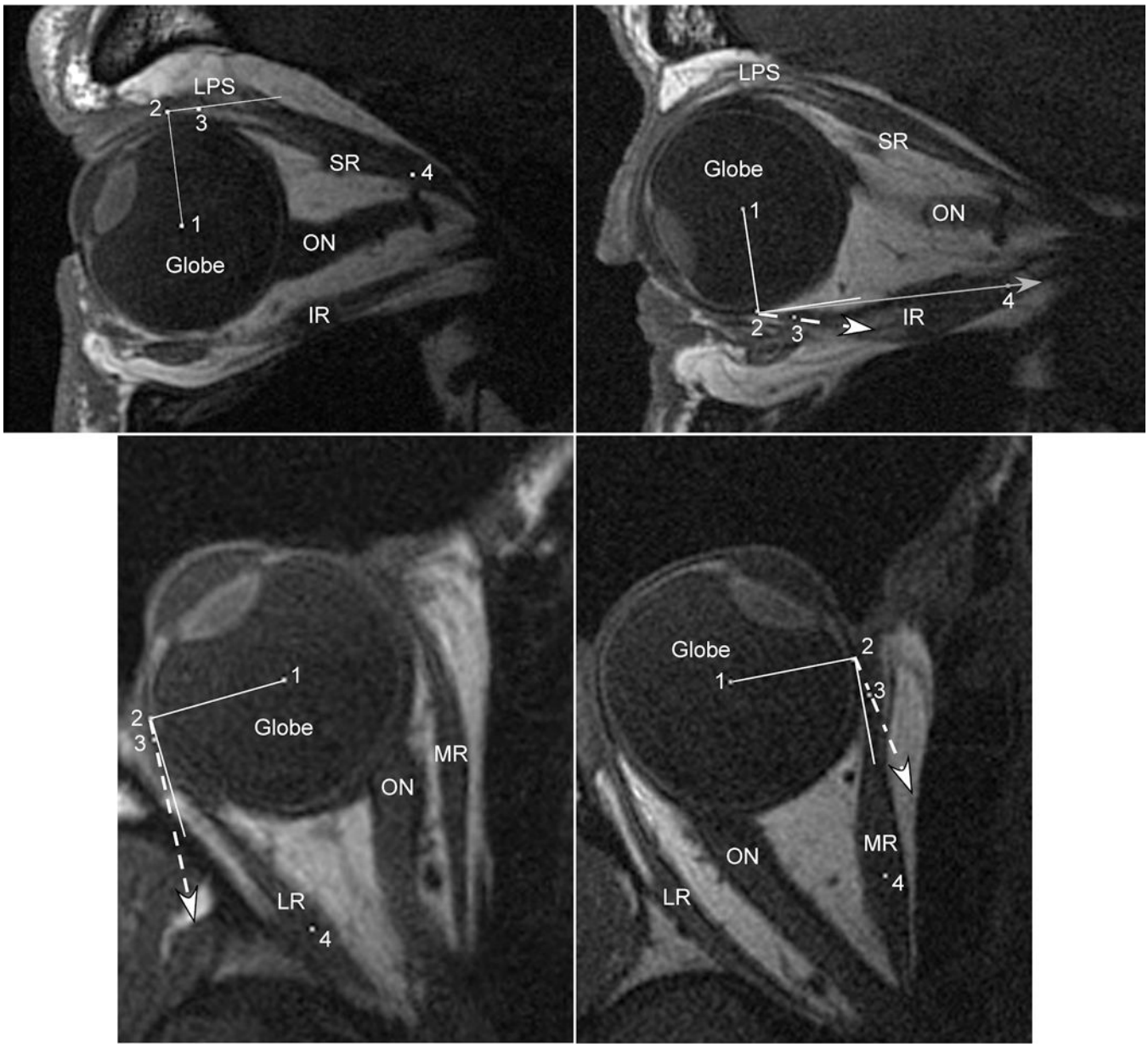

Figure 3.

Axial and quasi-sagittal magnetic resonance imaging (MRI) in normal subjects maintaining large ipsiversive ductions. For each panel, the solid white line represents a perfect tangent to the globe. The dashed white line with arrow represents the measured angle at tendon insertion. The solid gray line with arrow represents the predicted angle based on the “arc of contact” model. Point (1) marks the globe center, (2) the extraocular muscle insertion (EOM), (3) the middle of the immediate posterior tendon path, and (4) the middle of the posterior EOM belly. Upper Left) Supraduction. This sagittal MRI demonstrates the typical finding for the superior rectus (SR), perfect tangency for both the measured angle at tendon insertion and the predicted angle assuming an “arc of contact.” Because the line to point (4) created an angle less than 90°, the “arc of contact” measure was 0° (perfectly tangent) as the

SR wraps around the globe. Upper Right) Infraduction. This sagittal MRI of the inferior rectus (IR) demonstrates a much larger angle at tendon insertion than predicted because of inferior bowing of the IR path near its insertion. Even though the IR insertion (2) has not yet rotated posterior to globe center, the IR has experienced a substantial loss of tangency not predicted by the “arc of contact” model. Lower Left) Abduction. Similar to the SR, on axial MRI the “arc of contact” model predicts no loss of tangency for the lateral rectus (LR) during abduction. The thickness of the LR tendon, however is sufficient to create a small measured angle at its insertion. Lower Right) Adduction. Similar to the IR, on axial MRI the medial rectus (MR) demonstrates a much larger angle at tendon insertion than predicted by the “arc of contact” model because of tendon thickness and curvilinear MR path. Even though the MR insertion (2) remains anterior to globe center, the MR tendon has a substantial loss of tangency not predicted by its “arc of contact”. LPS = Levator Palpebrae Superioris; SR = Superior Rectus; IR = Inferior Rectus; LR = Lateral Rectus; MR = Medial Rectus; ON = Optic Nerve.

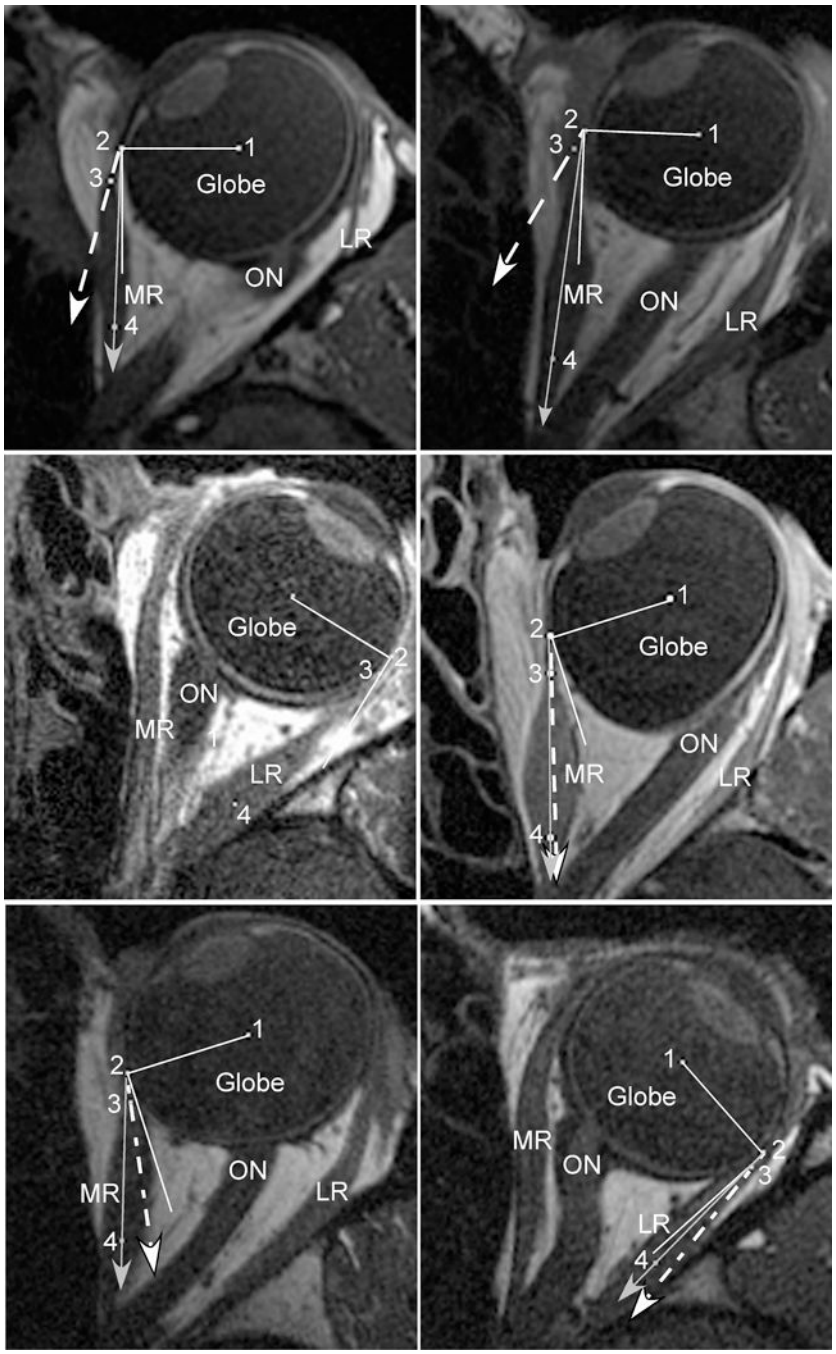

Fig. 4.

Axial magnetic resonance imaging (MRI) in strabismic subjects maintaining large ipsiversive ductions. In each panel, the solid white line represents a perfect tangent to the globe. The dashed white line with arrow represents the measured angle at tendon insertion. The solid gray line with arrow represents the predicted angle based on the “arc of contact” model. Point (1) marks the globe center, (2) the extraocular muscle insertion (EOM), (3) the middle of the immediate posterior tendon path, and (4) the middle of the posterior EOM belly. Upper Left) Subject with lateral rectus (LR) palsy. Because of the large esotropia

created by the palsy, the medial rectus (MR) insertion (2) is near the equator of the globe. In this position, however, the curvilinear MR path and thickened posterior belly creates a much larger loss of tangency than predicted by the “arc of contact” model. Upper Right) Subject who had undergone prior medial rectus (MR) resection. Similarly, after MR resection, the thickened insertion creates a much larger loss of tangency during adduction than predicted by the “arc of contact” model. Center Left) Subject who had undergone prior LR recession. The measured angle at tendon insertion demonstrates perfect tangency with the globe during abduction, identical to the “arc of contact” model. Center Right) Subject who had undergone prior MR recession. The measured angle at tendon insertion is nearly identical to the predicted angle from the “arc of contact” model. The combination of recession and adduction has rotated the insertion (2) posterior to globe center, plus the recessed MR has a thinned tendon and a nearly linear path towards its insertion, creating a near perfect agreement between predicted and measured angles. Lower Left) Subject who had undergone prior MR posterior fixation. Similar to MR recession, the posterior fixation suture has moved the effective MR insertion (2) posterior to globe center during adduction. Because the posterior muscle path deflects inward towards the center of the orbit, however, the measured angle at tendon insertion is closer to globe tangency than predicted. This MRI demonstrates the only scenario where the “arc of contact” model predicted a much greater loss of globe tangency than was actually measured. Lower Right) Subject who had undergone prior LR posterior fixation. The measured angle at tendon insertion was slightly larger than predicted by the “arc of contact” model, but the loss of tangency was much less than observed after MR posterior fixation. LR = Lateral Rectus; MR = Medial Rectus; ON = Optic Nerve

Table 1:
Normal Subjects Imaged During Large Ipsiversive Ductions

	# of Subjects	Globe Rotation (°)	Angle at Insert (°)		"Arc of Contact" Angle (°)		Paired T-Test
			Average	Range	Average	Range	
Medial Rectus	7	22.6	5.0	0.0 to 12.3	0.0 *	0.0 *	0.03
Lateral Rectus	5	27.6	4.9	0.0 to 7.7	0.0 *	0.0 *	0.02
Superior Rectus	11	26.2	0.6	0.0 to 3.6	0.0 *	0.0 *	0.04
Inferior Rectus	12	25.7	7.4	0.0 to 16.0	1.2	0.0 to 10.2	0.00003

Globe rotation is defined as rotation towards the scanned extraocular muscle, i.e. degrees of adduction for the medial rectus.

* "Arc of contact" predicted angles were 0 degrees (perfectly tangent) for every subject in this group.

Table 2 -

Clinical Profile of Horizontal Strabismus Subjects

Subject	Type of Strabismus	Horizontal Strabismus Surgery Performed (mm)			
		RMR	RLR	LMR	LLR
1	Esotropia	Recess 6.5	-	Recess 6.5	-
2	Esotropia	-	Resect 7.0	-	Resect 7.0
3	Exotropia	Resect 6.0	Recess 7.0	Resect 6.0	Recess 7.0
4	Exotropia	Resect 4.0	-	Resect 4.0	-
5	Exotropia	Resect 5.0	Recess 7.0	-	Recess 7.0

RMR = right medial rectus; RLR = right lateral rectus; LMR = left medial rectus; LLR = left lateral rectus

Table 3:
Strabismic Subjects Imaged During Large Ipsiversive Ductions

	# of Subjects	Globe Rotation (°)	Angle at Insert (°)		"Arc of Contact" Angle (°)		Paired T-Test
			Average	Range	Average	Range	
MR in LR Palsy	7	25.6	9.9	6.3 to 15.3	0.5	0.0 to 1.6	0.0007
MR Resection	4	23.1	9.0	0.0 to 18.5	1.2	0.0 to 6.1	0.02
MR Recession	1	35	15.2	-	17.2	-	-
LR Recession	2	31.5	2.9	0.0 to 5.9	0.0*	0.0*	-
MR Posterior Fixation	1	23.7	12.2	-	19.4	-	-
LR Posterior Fixation	1	38.4	9.3	-	3.4	-	-

Both lateral rectus (LR) recession subjects also underwent medial rectus (MR) resections and are counted in both groups. Globe rotation is defined as rotation towards the scanned extraocular muscle, i.e. degrees of adduction for the MR.

*"Arc of contact" predicted angles were 0 degrees (perfectly tangent) for every subject in this group.